

Engine oil exposure and performance degradation of composite brake pad based on natural materials

Sunardi SUNARDI ^{1,*}, Iman SAEFULOH ¹, Shofiatul ULA ¹, Dody ARIAWAN ², Eko SUROJO ², Aditya Rio PRABOWO ², Deni PURNOMO ³

¹ Universitas Sultan Ageng Tirtayasa, Cilegon, Indonesia

² Universitas Sebelas Maret, Surakarta, Indonesia

³ National Research and Innovation Agency, South Tangerang, Indonesia

*Corresponding author: sunardi@untirta.ac.id

Keywords

oil exposure
tribological properties
calcined eggshell
bamboo particle
brake pads
green materials

History

Received: 13-08-2025

Revised: 08-10-2025

Accepted: 20-10-2025

Abstract

Exposure to humid environments can influence the behaviour of the composite brake pad. The use of hazardous materials in brake pads poses health risks. Therefore, it is essential to utilise more environmentally friendly materials. The brake pads in this study, composed of 35 vol. % phenolic resin, 25 vol. % eggshell particles, 10 vol. % bamboo fibre, 5 vol. % bamboo particles, 10 vol. % alumina powder, 5 vol. % zinc powder and 10 vol. % graphite powder, underwent a rigorous manufacturing process involving cold compaction, hot compaction and post-curing. The samples were immersed in engine oil for 12, 24, 36 and 48 hours. The results of the study indicated that composites made from calcined eggshell and bamboo particles maintained their performance even after being exposed to engine oil. Following this exposure, the composites exhibited a coefficient of friction ranging from 0.33 to 0.36, a friction stability coefficient between 71.59 and 79.19, a flexural strength ranging from 7.23 to 8.25 MPa and a flexural strain ranging from 0.54 to 1.11 %. Additionally, the wear rate experienced a slight increase, measuring between 4.75 and 6.64 mm³/m. The flexural modulus was found to be between 4.44 and 5.49 GPa, while the hardness ranged from 43.35 to 91.05 HRR.

1. Introduction

Research on natural fibre degradation has the potential to significantly impact the field of materials science. The hygroscopic characteristics of natural fibres can trigger volumetric swelling [1], leading to changes in mechanical properties [2]. The composite degradation process is influenced by many factors, including the type of fibre, the matrix and the environmental conditions. Humid environmental conditions in polymer composites generally cause plasticity in epoxy and polyamides, which can reduce tensile strength, yield strength and modulus of elasticity [3]. The combination of water and heat exposure causes hygrothermal ageing, which triggers plasticisation, matrix

hydrolysis, matrix-fibre bond release, swelling, mass loss and chemical changes. A study conducted by Chiang et al. [4] showed that the volume fraction, filler size and soaking time affect the thickness expansion of the composite.

The literature on composites in water or humid environments is extensive. However, the effects of engine oil exposure on brake pad performance require further investigation. The infiltration of engine oil into the brake pad material can reduce its modulus of elasticity and hardness at the micro level [5]. Composites with oil-containing microcapsules show decreases in the coefficient of friction and the wear rate of up to 4 % and 0.25 %, respectively [6]. The presence of oil in the composite can form a lubricating layer that minimises direct contact between surfaces [7].

As sustainability issues gain importance, the utilisation of organic materials for eco-friendly brake



This work is licensed under a Creative Commons Attribution-NonCommercial 4.0 International (CC BY-NC 4.0) license

lining requires further investigation. Using natural materials like *Miscanthus* and cashew can help reduce density [8]. Additionally, incorporating 3 wt. % of blue *Cupressus arizonica* cones yields a high coefficient of friction [9]. The inclusion of rice husk ash particles can enhance the hardness of brake lining composites [10]. Research on epoxy composites reinforced with fibreglass and immersed in multigrade engine oil (SAE 15W-40) and extra-high-performance hydraulic brake fluid is crucial. This research highlights how these oils affect the flexural strength and flexural modulus of the composites [11]. Furthermore, air and oil absorption tend to increase with higher *Cortaderia selloana* content [12].

Literature review conducted by Sunardi et al. [13] showed that eggshell particles have the potential to be used as friction material ingredients. In further research, Sunardi et al. [14] stated that brake pad composites using 5 vol. % bamboo particles and 25 vol. % calcined eggshell particles as hybrid fillers can achieve optimal hardness and tribological properties. Utilisation of eggshells is an effort to develop environmentally friendly materials [15]. The addition of 6 wt. % eggshell particles as a filler in pineapple leaf fibre-reinforced composites can improve the mechanical properties. The combination of 5 vol. % copper powder and 15 vol. % glass powder in a composite reinforced with bamboo and coconut fibres has the lowest oil absorption capacity [17].

In this study, bamboo and calcined eggshell particles were used as hybrid fillers in brake pad composites. Oil exposure can affect the performance of brake pads. Therefore, this study will examine the impact of oil exposure on brake pads, as previous research has not extensively investigated these effects. This study aims to address these limitations.

2. Materials and methods

This research aims to utilise environmentally friendly materials in brake pad composites. Bamboo was chosen as a reinforcement and filler for the composite due to its ability to increase hardness and wear resistance [18]. Meanwhile, the use of eggshell particles as fillers is due to the ability to increase the dimensional stability [1] and enhance resistance to high temperatures [19].

2.1 Pre-treatment of materials

Eggshells are collected from household waste. They are first washed to remove dirt, then boiled in water for an hour. Afterwards, the eggshells are dried in the sun. The dried eggshells are crushed

and filtered through a 200-mesh sieve. The eggshell particles were analysed using a particle size analyser, which revealed an average particle size of 74.74 μm . Finally, the eggshell particles are calcined in a furnace at 900 °C for 2 hours. The calcination process results in a phase change of eggshell particles from CaCO_3 to CaO .

Bamboo fibres were obtained using the water retting method. The fibres were cut into pieces with an average length of 5 ± 1 mm and an average diameter of 110 ± 48 μm . Bamboo particles are obtained from bamboo processing artisans in various sizes and sieved to a maximum size of 297 μm . The separation of parenchyma from the bamboo particles was achieved by soaking them in water. Due to its low density, the parenchyma floats to the surface, where it can be discarded.

An alkali treatment was performed by soaking the bamboo fibres or particles in a 6 wt. % NaOH solution for 3 hours [20]. This concentration was chosen because it has been found to be effective in removing impurities and enhancing the surface properties of bamboo fibres. Following this, the bamboo was soaked in a silane solution. A 1 % vinyltrimethoxysilane solution was prepared by dissolving it in a mixture of ethyl alcohol and distilled water at an 80:20 volume ratio. After soaking, the bamboo fibres and particles were thoroughly washed with flowing distilled water until the pH reached 7 to remove unreacted silane molecules. The bamboos were then dried in the sun for two days and placed in an oven at 100 °C for 3 hours. Finally, the bamboo fibres and particles were stored in plastic bags to prevent water absorption from the atmosphere before being used to produce composite samples.

2.2 Manufacturing of composite

The composition of brake pads consists of various types of materials, and their functions are detailed in Table 1. This calculation is based on the volume fraction. The brake pad composite material mixture is first cold-compacted at a pressure of 40 MPa for 5 minutes [14]. This is followed by a crucial step of hot compaction at a temperature of 150 °C, a pressure of 40 MPa and a holding time of 10 minutes. It is during this step that chemical bonds are formed, playing a significant role in the final product. The next step is post-curing, which involves heating the sample continuously from ambient temperature to 180 °C for 420 minutes. After the curing process, the electric oven is opened and the sample is allowed to cool under ambient air.

Table 1. Composition of organic brake pad

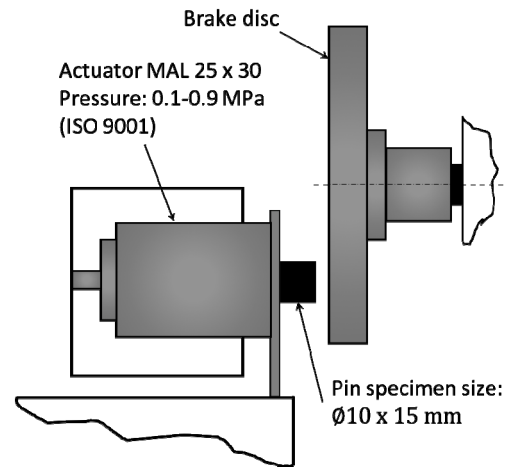
Material	Function	Amount, vol. %
Phenolic	matrix	35
Eggshell particles	filler	25
Bamboo fibres	reinforcement	10
Bamboo particles	filler	5
Alumina	friction modifier	10
Zinc	friction modifier	5
Graphite	solid lubricant	10

2.3 Material characterisation

The composite samples were immersed in Federal Ultratec SAE 20W-50 engine oil, API SJ, for durations of 12, 24, 36 and 48 hours. The engine oil specifications used have a density of 880 kg/m³ at 15 °C, kinematic viscosities of 18 and 150.8 mm²/s at 100 and 40 °C, respectively, a viscosity index of 133, a flash point of 227 °C and a pour point of −30 °C. The sample coding is as follows: Control is the composite sample that was not exposed to engine oil, and EO-12, EO-24, EO-36 and EO-48 are composite samples immersed in engine oil for 12, 24, 36 and 48 hours, respectively.

Oil absorption was measured according to the ASTM D570 standard to evaluate its effects on the mechanical and tribological properties of the brake pad composition. To determine the rate of oil absorption, the brake pad composite was immersed in engine oil for varying periods, specifically for 12, 24, 36 and 48 hours. Prior to immersion, the sample was weighed using a digital balance with an accuracy of 0.001 g. After the specified immersion duration, the sample was removed and the excess oil was cleaned off using a soft cloth designed for quick oil absorption. The sample was then weighed again to calculate the percentage of oil absorption.

The coefficient of friction was measured in pin-on-disc testing, conducted at a contact pressure of 0.75 MPa and a sliding speed of 12 m/s. The disc was made from DIN X153CrMoV12 steel, with a hardness of 45 HRC and an average surface roughness (*Ra*) ranging from 0.43 to 1.37 µm. Data recording was carried out during a sliding distance of 6020.76 m. The sample pin for the tribology test has a diameter of 10 mm and a length of 15 mm. With a contact pressure of 0.75 MPa, the normal force on the pin surface is 58.875 N. The pin-on-disc test equipment setup is shown in Figure 1.

**Figure 1.** Setup of the pin-on-disc test equipment

Before starting each test, the disc surface is cleaned with a soft cloth to remove any dirt. The friction force between the sample and disc surfaces is then recorded using a data acquisition system (Advantech USB-4716). Each test is conducted by replicating the procedure five times.

The friction stability coefficient (FSC) is used as a parameter that measures how stable the coefficient of friction remains over time at the interface between the disc and the brake pad. Materials giving a high FSC demonstrate better stability in their coefficients of friction, making them ideal for use as brake lining materials. On the other hand, those giving a low FSC need improvements in the performance as the brake lining material. Equation (1) can be used to calculate the FSC in % [21].

$$FSC = \frac{\mu_{ave}}{\mu_{max}} 100, \quad (1)$$

where μ_{ave} is the average coefficient of friction over the same period and μ_{max} is the maximum coefficient of friction in that same period.

Wear rate was measured after a sliding distance of 6020.76 m for each test. It was obtained by dividing the wear volume by the contact load and the sliding distance.

Flexural strength is the ability of a material to withstand bending loads without breaking. The sample size used is 100 × 10 × 4 mm. The flexural test is conducted in accordance with ASTM D790 standard using the three-point bending method.

The test was carried out on a Zwick tensile tester Z020 with an initial load of 0.2 N and a test speed of 2 mm/min. Five replications were carried out to obtain accurate data. Equation (2) determines the magnitude of the flexural strength σ in MPa.

$$\sigma = \frac{3P_{\max}L}{2bh^2}, \quad (2)$$

where P_{\max} is the maximum load at the fracture point in N, L is the support span length in mm and b and h are the width in mm and thickness of specimen in mm, respectively.

Flexural strain indicates the relative deformation of the material when a load is applied. In this study, flexural strain ε in mm/mm is defined as in Equation (3).

$$\varepsilon = \frac{6Dh}{L^2}, \quad (3)$$

where D is the deflection in the middle of the beam span in mm, h is the thickness of the specimen in mm and L is the support span length in mm.

Composite hardness testing was performed with five replications to obtain accurate data. Composite hardness testing was carried out using Rockwell hardness type R, and the testing machine used was a Zwick Roell hardness tester.

The surface roughness of the worn pin was measured using a Mitutoyo Surftest SJ-310 portable surface roughness tester. The testing was conducted in accordance with JIS B 0601 standard. The sampling length and number of sampling lengths were 0.8 mm and 5, respectively. The stylus used was a standard diamond tip with a 2 μm radius. The testing parameters were a transverse measurement speed of 0.50 mm/s and a return speed of 1 mm/s with a total sampling length of 4 mm. The surface roughness parameter analysed in this study was the arithmetical mean deviation R_a , measured in microns. Surface roughness of the worn surfaces is measured in two directions: the x-direction, parallel to the sliding direction and the y-direction, perpendicular to it.

The worn surface morphology of a pin was examined using a scanning electron microscope (SEM) and energy-dispersive spectroscopy (EDS) at Politeknik ATMI Surakarta. Surface morphology images were taken using a Carl Zeiss EVO 10 SEM with magnifications of 500 \times .

3. Results and discussion

This study aimed to evaluate the effect of prolonged exposure to engine oil on the mechanical and tribological properties of composites by immersing them in the oil. The immersion duration, set at 12, 24, 36 and 48 hours, had an impact on the performance of the composite materials.

3.1 Oil absorption

Table 2 presents the percentage of oil absorbed after immersion of the composite samples. The percentage of oil absorption tends to increase with immersion duration in engine oil.

Table 2. Oil absorption

Immersion duration, h	Oil absorption, %
12	1.256 \pm 0.221
24	1.547 \pm 0.231
36	1.688 \pm 0.199
48	1.935 \pm 0.182

3.2 Functional groups of atomic bonds

Figure 2 presents the composite FTIR (Fourier transform infrared spectroscopy) spectrum before and after immersion in the engine oil for 12, 24, 36 and 48 hours. After immersing the sample in engine oil, the peak at 3641 cm^{-1} corresponds to the stretching vibration of the $-\text{OH}$ bond, which is characteristic of the hydroxyl group from water molecules on the surface of the CaO particle, alcohols and phenols. Notably, the $-\text{OH}$ stretching has not been noticed in the sample that was not exposed to engine oil. In this sample, a wide band is noticed in the range between 3641 and 2951 cm^{-1} , which is associated with free hydroxyl groups. This band vanished after exposure to engine oil. The exposure lasted up to 48 hours and revealed the transmittance of its hydroxyl ($-\text{OH}$) bonds.

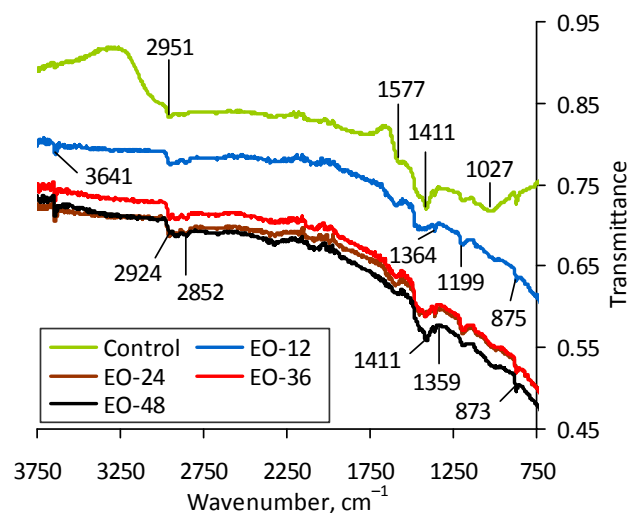


Figure 2. FTIR of composite brake pads after various engine oil immersion durations

The peaks at 2852 and 2924 cm^{-1} indicate asymmetric stretching of the $-\text{CH}$ bond. This peak indicates the presence of methyl ($-\text{CH}_3$) or methylene ($-\text{CH}_2$) groups, which are generally derived from organic compounds. The peak at

1577 cm^{-1} corresponds to C=C stretching and indicates an aromatic ring vibration [22]. The peak intensity of eggshell particles noticed at 1411 cm^{-1} is characteristic of the C–O bond, which is strongly associated with calcium oxide minerals. The bands at 1359 and 1364 cm^{-1} indicate the presence of C–H bonds, suggesting the presence of methyl and CH_3 groups.

The peak at 1199 cm^{-1} exhibits strong absorption intensity, corresponding to the C–O stretching vibration, indicating the presence of phenolic C–O groups. Bamboo fibres and particles treated with alkali and silane can be identified by the C–O stretching vibration peaks of alcohol, the aromatic C–H in-plane deformation and the C=O peak at 1027 cm^{-1} . Finally, the peaks at 873 and 875 cm^{-1} indicate the presence of CaO particles associated with C–O bonds, suggesting the carbonation of calcium oxide.

3.3 Coefficient of friction behaviour

Figure 3 shows the coefficient of friction values after exposure to engine oil. It was found that exposure to engine oil had no significant effect on the coefficient of friction. Before exposure to the engine oil, the coefficient of friction was 0.32, and after exposure, it increased and was in the range from 0.33 to 0.36.

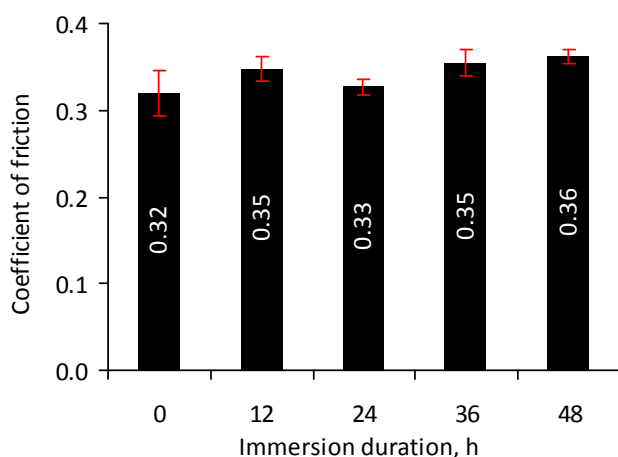


Figure 3. Coefficient of friction values after various engine oil immersion durations

Calcium oxide, when exposed to water from air or engine oil, undergoes a hydration process that results in the formation of a cement-like material. The primary products of this reaction are calcium silicate hydrate and calcium hydroxide. This condition is confirmed by FTIR data, which shows bands at 3641, 1411, 875 and 873 cm^{-1} . During hydration, a porous structure develops, which retains the water needed for further hydration. This

process creates a hardened and textured surface layer. The rough surface contributes to a high coefficient of friction. Moreover, the amount of engine oil on the composite surface decreases as the contact temperature at the interface between the brake pad and disc rises. Despite this decrease, the coefficient of friction remains high. These results are consistent with those of Jasim et al. [23], who stated that increasing the cement content by up to 20 wt. % leads to an increase in the composite's surface roughness. As the surface roughness increases, the coefficient of friction also increases.

If the water content continues to increase and the coefficient of friction reaches its maximum value, boundary lubrication occurs, causing a decrease in the coefficient of friction [24]. The presence of bamboo particles and fibres affects the coefficient of friction, the friction stability coefficient and the wear rate. Yu et al. [25] showed that the addition of bamboo fibres can increase the coefficient of friction and the material's friction stability, while also reducing the wear rate.

Figure 4 shows the friction stability coefficient of the samples after exposure to the engine oil. The friction stability of the samples remained relatively stable, except for the EO-24 sample, which experienced a significant decrease in its friction stability coefficient. This decrease is supported by the coefficient of friction profile, which displayed noticeable fluctuations.

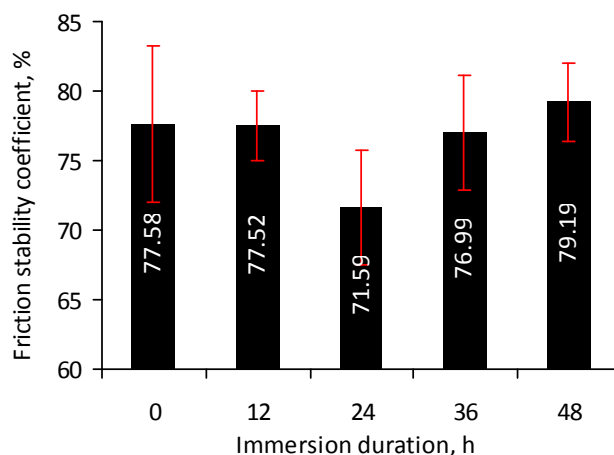


Figure 4. Friction stability coefficient values after various engine oil immersion durations

The friction stability coefficient (FSC) remains relatively stable, ranging from 76.99 to 79.19 %. However, the composite sample exposed to engine oil for 24 hours induced a significant decrease, obtaining an FSC of only 71.59 %. This reduction is attributed to the average coefficient of friction value after reaching the steady-state condition of 0.33, since during initial contact between the brake pad

and the disc, the coefficient of friction reaches 0.46 within the first 100 seconds, as illustrated in Table 3.

Table 3. Average and maximum coefficient of friction values

Sample	μ_{ave}	μ_{max}	Difference
Control	0.32	0.41	0.09
EO-12	0.35	0.45	0.10
EO-24	0.33	0.46	0.13
EO-36	0.35	0.46	0.11
EO-48	0.36	0.46	0.10

Figure 5 shows the coefficient of friction profiles after samples were exposed to engine oil at various engine oil immersion durations. These profiles correspond to the wear rate of the composite samples. Exposure to engine oil does not significantly affect its tribological behaviour. The samples immersed in engine oil exhibited a good FSC.

The coefficient of friction when the hydraulic oil was between the composite surface and the disc decreased significantly compared to dry sliding conditions [26]. This study demonstrates that the use of calcined eggshell particles and bamboo particles is predicted to maintain the tribological properties of brake pads even when exposed to engine oil over an extended period. To confirm the contribution of calcined eggshell particles and bamboo, an investigation and comparison with composite materials that do not use these materials is necessary.

Figure 5a presents the coefficient of friction profile when a brake pad composite was not exposed to engine oil, with an FSC of 77.58 %. The profile shows that the coefficient of friction stabilises 150 seconds after the initial contact between the brake pad and disc surfaces. When the composite was exposed to engine oil for 12, 36 and 48 hours, the FSC values were 77.52, 76.99 and 79.19 %, respectively, as illustrated in Figures 5b, 5d and 5e. The lowest FSC value of 71.59 % occurs when the composite was exposed to engine oil for 24 hours, as shown in Figure 5c.

The hardness of the brake pad composite influences the FSC value of each sample. As contact time between the brake pad composite and the disc increases during testing, the film formed by engine oil diminishes. Moreover, the frictional heat generated at the interface between the brake pad and disc surfaces further reduces the amount of engine oil that diffuses into the composite material.

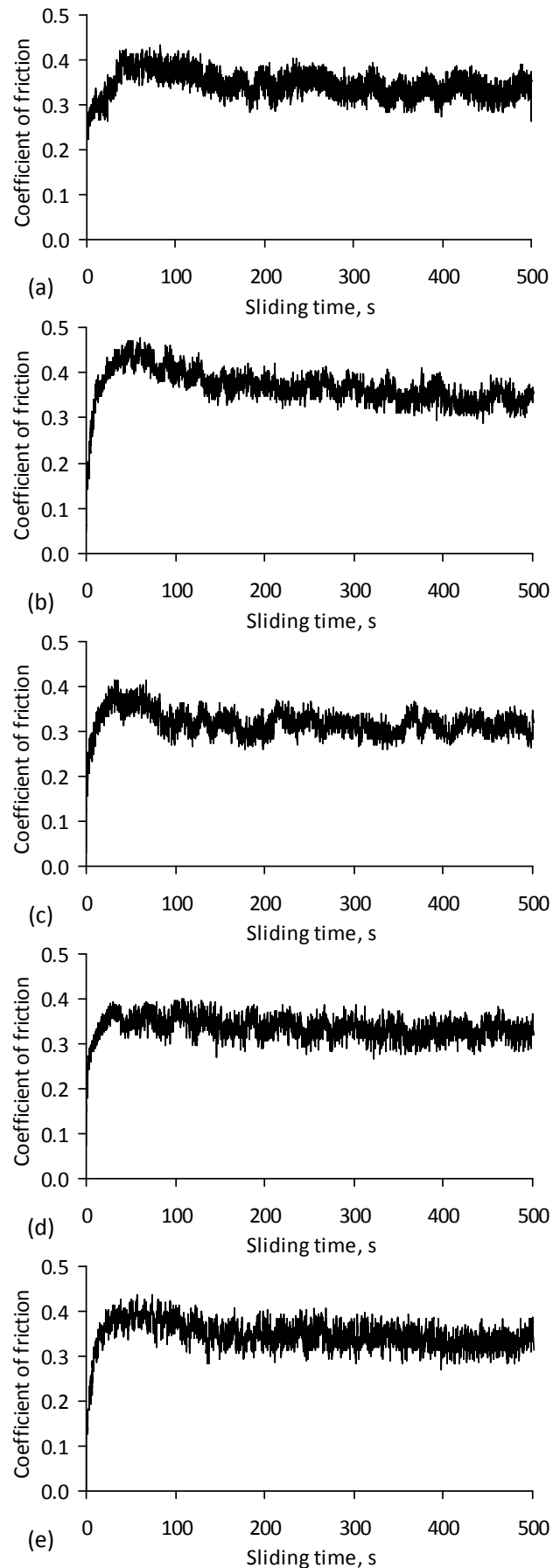


Figure 5. Coefficient of friction profiles after various engine oil immersion durations: (a) not exposed, (b) 12 hours, (c) 24 hours, (d) 36 hours and (e) 48 hours

3.4 Wear rate

Figure 6 illustrates the wear rate of brake pad composites that were exposed to engine oil over various immersion durations. Generally, wear rate values and their standard deviations indicate that oil exposure tends to increase wear rate, although the increase remains within the range of the standard deviations. However, exposure to engine oil for 12 hours caused a significant increase in the wear rate. A significant reduction in the hardness of the sample after 12 hours of exposure to engine oil contributed to this increase in wear rate. The wear rate of the control sample was $4.43 \text{ mm}^3/\text{m}$. The amount of engine oil on the composite surface will decrease and may even evaporate due to the heat generated at the brake pad-disc interface. This condition is characterised by an increase in wear volume on the composite compared to the control composite.

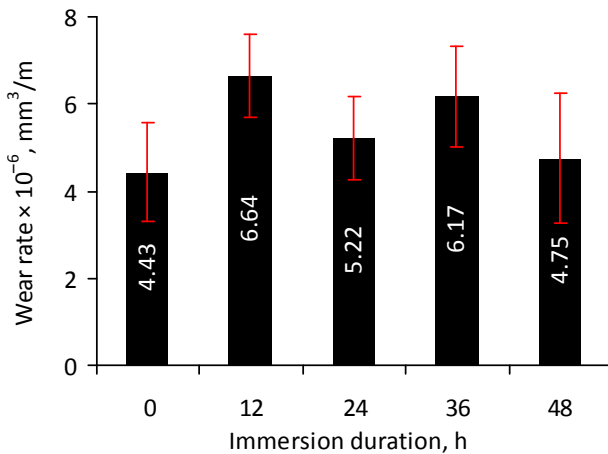


Figure 6. Effect of immersion duration on wear rate of composite brake pads

The wear rate of brake pad samples increases with increasing coefficient of friction. Research by Khun and Liu [27] showed different results, where the width and depth of the wear track decreased with increasing immersion duration. The lower coefficient of friction of the materials caused this decrease. The decrease in the wear rate of brake pads after immersion in engine oil is due to the uniform film layer that protects the brake pad contact surface, reducing contact stress and local temperature increases [28]. Polymer composites filled with lubricant-containing microcapsules form a lubricating layer on the contact surface, allowing them to withstand high loads [29]. A comparison of tribological properties after exposure to various immersion durations in engine oil is presented in Table 4.

The roughness of the worn surfaces after undergoing pin-on-disc testing is shown in Figure

7. The research reveals that prolonged exposure to engine oil tends to decrease the roughness of the composite brake pad sample, a result that challenges existing assumptions about the effects of oil on wear.

Table 4. Tribological properties

Property	Immersion duration, h				
	0	12	24	36	48
Coefficient of friction	0.32	0.35	0.33	0.35	0.36
Wear rate $\times 10^{-6} \text{ mm}^3/\text{m}$	4.43	6.64	5.22	6.17	4.75
Friction stability coefficient, %	77.58	77.52	71.59	76.99	79.19

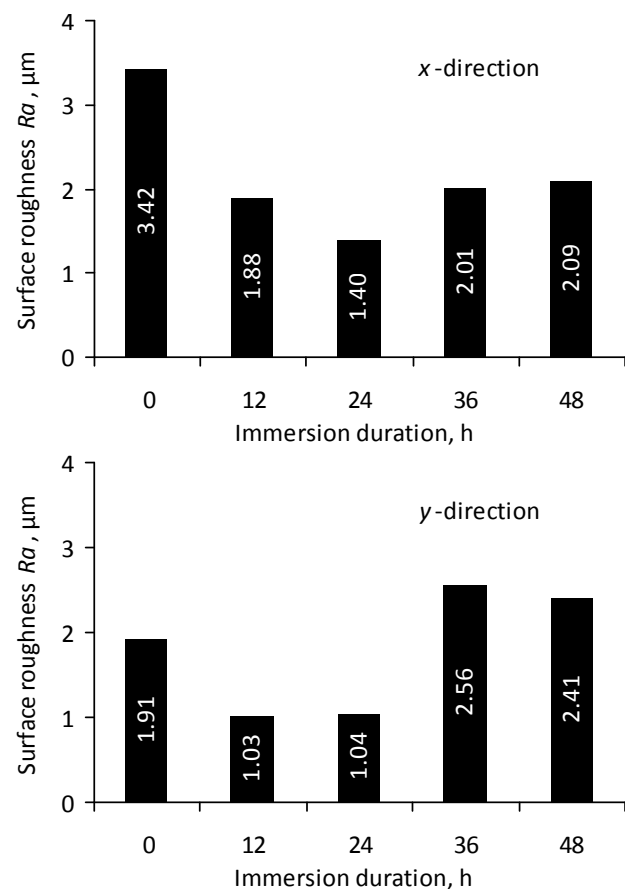


Figure 7. Effect of immersion duration on worn surface roughness of composite brake pads

3.5 Mechanical properties

Figure 8 illustrates the relationship between immersion duration and the flexural strength of the composite samples. The average flexural strength of the composites that were not immersed in engine oil was 6.68 MPa. After immersion in the engine oil, the flexural strength increased for up to 24 hours of exposure. However, after this period, the flexural strength began to decrease. This suggests that

exposure to engine oil did not cause any degradation in flexural strength. There was a slight increase in flexural strength of the composite, which is attributed to the initial treatment of the fibre with a combination of alkali and silane and the formation of cement hydration. The presence of ethanol during the silane treatment significantly enhances the tensile strength of the bamboo fibres [30]. FTIR data reveal that at 1411 cm^{-1} , the control sample shows a clear peak, which then disappears and reappears distinctly in the EO-48 sample. The peak at 1411 cm^{-1} indicates an intense stretching of the C–O bond. This explains why the flexural strength of the composite increases after exposure to engine oil but decreases after 48 hours of exposure. This reduction in flexural strength is shown by FTIR data, evidenced by a decrease in the peak at 1577 cm^{-1} , indicating a lower intensity of the C=C bond.

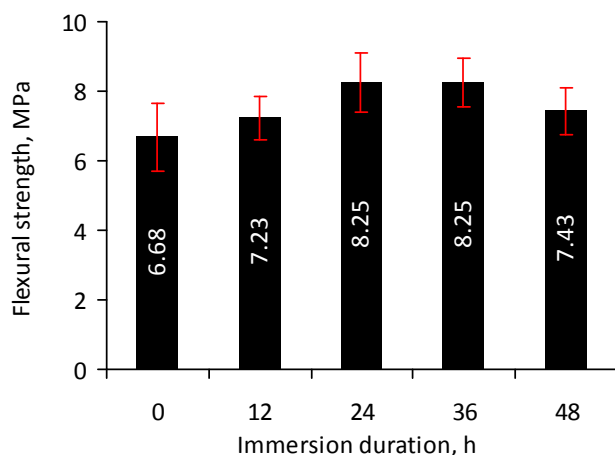


Figure 8. Effect of immersion duration on flexural strength of composite brake pads

Syahrani et al. [31] found that the immersion time of the composite did not significantly affect the degradation of its mechanical properties. This finding has important implications for the use and maintenance of composite materials. Another study showed that oil did not significantly affect the hardness and flexural strength of the composite, a result that underscores the complex relationship between fluid properties and composite behaviour [32].

The resistance of a material to flexural deformation is expressed by its flexural modulus. Figure 9 shows the correlation between the immersion duration of the composite and its flexural modulus. The flexural modulus decreased with immersion duration up to 24 hours, then increased again at 36 and 48 hours. The flexural modulus of the composite is inversely proportional to its flexural strength. This condition indicates

that the composite exposed to engine oil can still maintain its performance.

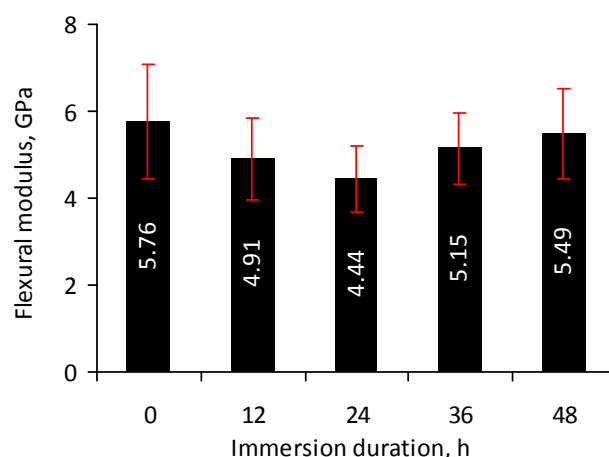


Figure 9. Effect of immersion duration on flexural modulus of composite brake pads

Flexural strain increases with the immersion duration, reaching a peak at 24 hours, after which it begins to decrease, as shown in Figure 10. This increase in flexural strain was also indicated by a decrease in the composite's flexural modulus and hardness. This condition differs from that reported by Afzal et al. [33], where the composite flexural strain decreased with ageing time for pure water, seawater and saltwater immersion media. Immersion of the composite in distilled water caused more severe damage than in other types of water.

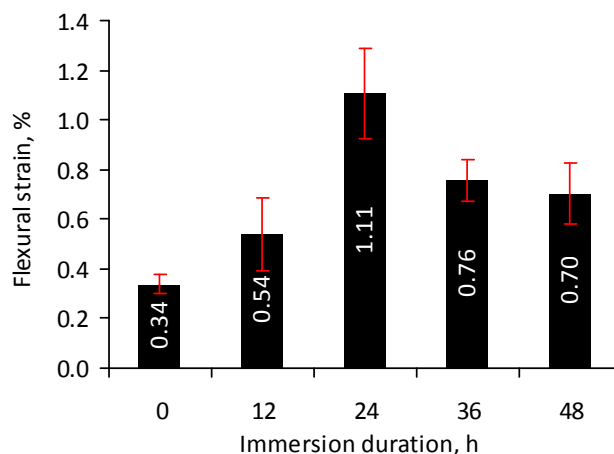


Figure 10. Effect of immersion duration on flexural strain of composite brake pads

The strain of the composite without exposure to engine oil was 0.338 %. After immersion in engine oil, the composite experienced a significant increase in strain. Halder et al. [34] showed that the flexural strain of the composite aged in seawater exceeded that of the dry sample. The same phenomenon was also stated in the study by Nosbi et al. [35], where the flexural strain increased after

immersion of the composite in distilled water for up to 14 days and then decreased. The interaction of composites with oil, a process that enhances the mechanical properties of the composite by increasing macromolecular mobility and causing solid-state reorganisation of the amorphous domains [36], underscores the crucial role of accurate matrix selection in achieving optimum composite performance. For instance, carbon fibre-reinforced polyethylene terephthalate glycol exhibits an intriguing pattern of increased tensile strength after up to 7 days of exposure to mineral engine oil, followed by a decline. This variability in response to oil exposure requires further research. In contrast, polylactide shows a consistent decrease in tensile strength with exposure duration [37].

In general, the hardness of composite brake pads decreases after exposure to engine oil. The hardness of the unexposed brake pad is 94.25 HRR. Amaro et al. [38] stated that hardness decreases when the samples are immersed in oil. This decrease is due to the plasticisation effect and the inability to withstand indentation. The reduction in composite hardness decreases with increasing immersion duration.

Figure 11 shows that the hardness of the composite decreases to a minimum after exposure to engine oil for 24 hours and then increases. Immersion of the composite in engine oil or hydraulic brake fluid shows an increase in hardness after immersion for 15 and 30 days [39]. The results of the study are in line with those of Mohammed and Issa [40], who reported that the hardness of unsaturated polyester resin composites decreased with increasing water exposure time. The results of mechanical testing on the composite exposed to engine oil are presented in Table 5.

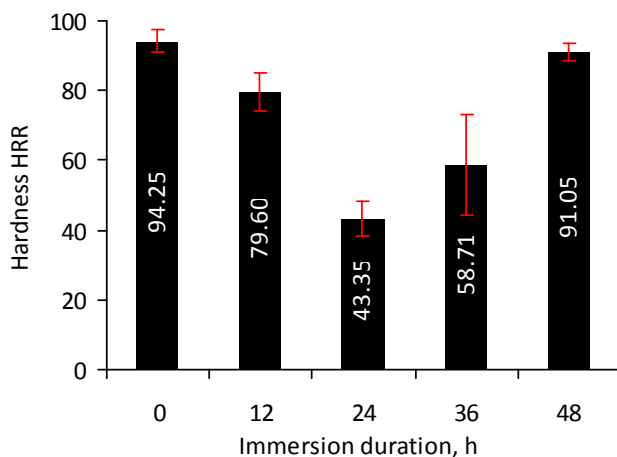


Figure 11. Effect of immersion duration on hardness of composite brake pads

Table 5. Mechanical properties

Property	Immersion duration, h				
	0	12	24	36	48
Flexural strength, MPa	6.68	7.23	8.25	8.25	7.43
Flexural modulus, GPa	5.76	4.91	4.44	5.15	5.49
Flexural strain, %	0.34	0.84	1.11	0.76	0.70
Hardness HRR	94.25	79.60	43.35	58.71	91.05

3.6 Worn surfaces morphology

Figure 12 illustrates the morphology of the worn surface of the samples after oil exposure. The worn surface of the EO-24 sample shows signs of adhesive wear, while the wear marks on the EO-36 sample are less pronounced. This difference in the appearance of worn surfaces is related to the hardness of the two samples. After exposure to engine oil, the EO-24 composite displayed a smoother surface, with an average surface roughness of 1.40 μm in the x-direction and 1.04 μm in the y-direction, as shown in Figure 7. This smoothness was supported by the sample's coefficient of friction, which was the lowest among all tested samples. Additionally, the low wear rate further confirmed the relatively smooth surface, as shown in Figure 12a.

In contrast, the EO-36 composite displayed average surface roughness values of 2.01 μm in the x-direction and 2.56 μm in the y-direction. SEM images indicated that this composite had a significantly rougher surface compared to the others. This rough surface was correlated with its high hardness, which resulted in a relatively high coefficient of friction of 0.35.

The wear patterns observed on the EO-24 sample indicate adhesive wear. This type of wear is characterised by wear debris from the primary plateau filling the surrounding valleys, which leads to the formation of secondary plateaus, as illustrated in Figure 12a. As a result, the EO-24 sample has a smoother surface compared to the EO-36 sample. In contrast, the EO-36 sample shows minimal wear traces. This difference in the appearance of worn surfaces is reflected in the hardness measurements, with the EO-36 sample reaching 58.71 HRR, while the EO-24 sample has a hardness of only 43.35 HRR.

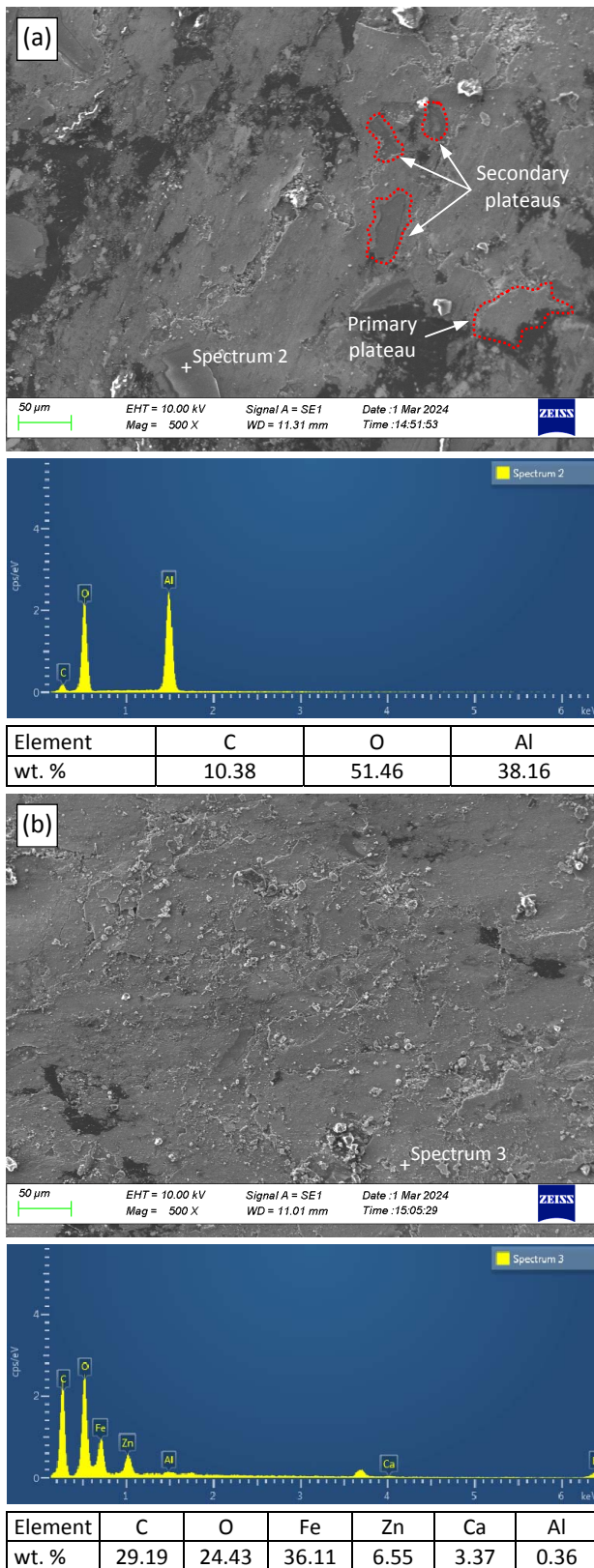


Figure 12. Morphology of the composite worn surface after exposure to engine oil for: (a) 24 hours and (b) 36 hours

The increased hardness in EO-36 can be attributed to more uniform cement hydration that occurs in samples exposed to engine oil for a longer duration, as illustrated in Figure 12b. Furthermore,

the presence of calcined eggshell particles in a humid environment enhanced the tribological performance of the composites. The immersion duration in lubricating oil also positively impacted the composite's flexural strength and ductility, while causing a slight decrease in its flexural modulus.

4. Conclusion

Exposure to engine oil affects the performance of composite brake pads, and several conclusions can be drawn.

Samples exposed to engine oil formed O–H hydroxyl bonds, which affected the mechanical and tribological properties of the composite. Samples exposed to engine oil maintained the coefficient of friction values. However, the wear resistance and the friction stability coefficient tended to decrease compared to the control sample.

The significant increase in flexural strength and flexural strain, along with the decrease in flexural modulus, suggests potential improvements in the durability and flexibility of the composite brake pads.

To assess whether adding calcined eggshell and bamboo particles enhances the mechanical and tribological properties of brake pads, an investigation is needed. This study will compare composites containing both calcined eggshell and bamboo particles to composites that do not include these natural materials, focusing on different composition ratios. Future research using uncalcined eggshell particles is warranted to determine differences in mechanical and tribological behaviour. The investigation into the viscosity of engine oil or other oils that frequently come into contact with brake pads needs further exploration.

Acknowledgement

This research is supported by the Directorate of Research and Community Service (DPPM) within the Ministry of Higher Education, Science, and Technology, Regular Fundamental Research (PFR) Scheme, Contract Number: 111/C3/DT.05.00/2025.

References

- [1] S. Sunardi, D. Ariawan, E. Surojo, A.R. Prabowo, C.H. Wibowo, H.I. Akbar, A. Sudrajad, H. Seputro, Dimensional stability of brake pads reinforced with calcined eggshell particles under exposed to engine lubricating oil, BIO Web of Conferences, Vol. 146, 2024, Paper 01058, DOI: [10.1051/bioconf/202414601058](https://doi.org/10.1051/bioconf/202414601058)

- [2] Y. Huang, M.T.H. Sultan, F.S. Shahar, R. Grzejda, A. Łukaszewicz, Hybrid fiber-reinforced biocomposites for marine applications: A review, *Journal of Composites Science*, Vol. 8, No. 10, 2024, Paper 430, DOI: [10.3390/jcs8100430](https://doi.org/10.3390/jcs8100430)
- [3] K.S. Randhawa, A. Patel, The effect of environmental humidity/water absorption on tribo-mechanical performance of polymers and polymer composites – A review, *Industrial Lubrication and Tribology*, Vol. 73, No. 9, 2021, pp. 1146-1158, DOI: [10.1108/ILT-02-2021-0045](https://doi.org/10.1108/ILT-02-2021-0045)
- [4] T.C. Chiang, M.S. Osman, S. Hamdan, Water absorption and thickness swelling behavior of sago particles urea formaldehyde particleboard, *International Journal of Science and Research*, Vol. 3, No. 12, 2014, pp. 1375-1379.
- [5] P.G. Ivanochkin, K.N. Dolgoplov, S.A. Danilchenko, Creation of oil-filled composites of tribotechnical purpose based on aromatic polyamide Phenylone C-2, *Solid State Phenomena*, Vol. 284, 2018, pp. 14-19, DOI: [10.4028/www.scientific.net/SSP.284.14](https://doi.org/10.4028/www.scientific.net/SSP.284.14)
- [6] L. Zhang, G. Xie, S. Wu, S. Peng, X. Zhang, D. Guo, S. Wen, J. Luo, Ultralow friction polymer composites incorporated with monodispersed oil microcapsules, *Friction*, Vol. 9, No. 1, 2021, pp. 29-40, DOI: [10.1007/s40544-019-0312-4](https://doi.org/10.1007/s40544-019-0312-4)
- [7] K. Chen, Y. Tang, Research progress on the design of surface texture in tribological applications: A mini-review, *Symmetry*, Vol. 16, No. 11, 2024, Paper 1523, DOI: [10.3390/sym16111523](https://doi.org/10.3390/sym16111523)
- [8] M. Unaldi, R. Kus, The effect of the brake pad components to the some physical properties of the ecological brake pad samples, *IOP Conference Series: Materials Science and Engineering*, Vol. 191, 2017, Paper 012032, DOI: [10.1088/1757-899X/191/1/012032](https://doi.org/10.1088/1757-899X/191/1/012032)
- [9] H. Yavuz, Evaluation of blue *Cupressus arizona* cone in automotive brake pad biocomposite, *BioResources*, Vol. 18, No. 3, 2023, pp. 5182-5197, DOI: [10.15376/biores.18.3.5182-5197](https://doi.org/10.15376/biores.18.3.5182-5197)
- [10] İ. Sugözü, H. Kuş, A. Avcu, Effects of rice husk ash particles on tribological properties of bronze matrix composite brake pads, *Science of Sintering*, Vol. 57, No. 3, 2025, pp. 369-387, DOI: [10.2298/SOS2410210455](https://doi.org/10.2298/SOS2410210455)
- [11] A.M. Amaro, P.N.B. Reis, M.A. Neto, C. Louro, Effect of different commercial oils on mechanical properties of composite materials, *Composite Structures*, Vol. 118, 2014, pp. 1-8, DOI: [10.1016/j.compstruct.2014.07.017](https://doi.org/10.1016/j.compstruct.2014.07.017)
- [12] H. Yavuz, H. Bayrakçeken, E. Çengelci, T.A. Arslan, An investigation on the performance of vehicle brake pads developed from *Cortaderia selloana* based biomass, *Biomass Conversion and Biorefinery*, Vol. 15, No. 4, 2025, pp. 5293-5302, DOI: [10.1007/s13399-023-05262-x](https://doi.org/10.1007/s13399-023-05262-x)
- [13] S. Sunardi, D. Ariawan, E. Surojo, A.R. Prabowo, H.I. Akbar, B. Cao, H. Carvalho, Assessment of eggshell-based material as a green-composite filler: Project milestones and future potential as an engineering material, *Journal of the Mechanical Behavior of Materials*, Vol. 32, 2023, Paper 20220269, DOI: [10.1515/jmbm-2022-0269](https://doi.org/10.1515/jmbm-2022-0269)
- [14] S. Sunardi, D. Ariawan, E. Surojo, A.R. Prabowo, H.I. Akbar, A. Sudrajad, H. Seputro, Optimization of eggshell particles to produce eco-friendly green fillers with bamboo reinforcement in organic friction materials, *Reviews on Advanced Materials Science*, Vol. 62, 2023, Paper 20230111, DOI: [10.1515/rams-2023-0111](https://doi.org/10.1515/rams-2023-0111)
- [15] B. Ngayakamo, A.P. Onwualu, Recent advances in green processing technologies for valorisation of eggshell waste for sustainable construction materials, *Heliyon*, Vol. 8, No. 6, 2022, Paper e09649, DOI: [10.1016/j.heliyon.2022.e09649](https://doi.org/10.1016/j.heliyon.2022.e09649)
- [16] Y. Ma, S. Shen, J. Tong, W. Ye, Y. Yang, J. Zhou, Effects of bamboo fibers on friction performance of friction materials, *Journal of Thermoplastic Composite Materials*, Vol. 26, No. 6, 2013, pp. 845-859, DOI: [10.1177/0892705712461513](https://doi.org/10.1177/0892705712461513)
- [17] I. Risyuma, M. Fitri, Analysis of oil absorption and friction coefficient of bamboo powder, coconut powder, glass powder, and copper powder composites for clutch pads, *International Journal of Innovation in Mechanical Engineering and Advanced Materials*, Vol. 4, No. 2, 2022, pp. 58-65, DOI: [10.22441/ijimeam.v4i2.18235](https://doi.org/10.22441/ijimeam.v4i2.18235)
- [18] Y. Sukrawan A. Hamdani S.A. Mardani, Effect of bamboo weight faction on mechanical properties in non-asbestos composite of motorcycle brake pad, *Materials Physics and Mechanics*, Vol. 42, No. 3, 2019, pp. 367-372, DOI: [10.18720/MPM.4232019_12](https://doi.org/10.18720/MPM.4232019_12)
- [19] S. Sunardi, D. Ariawan, E. Surojo, A.R. Prabowo, T. Ghanbari-Ghazijahani, C. Wibowo, H.I. Akbar, Tribological performance of polymer composite modified with calcined eggshell particles post high-temperature exposure, *Emerging Science Journal*, Vol. 8, No. 4, 2024, pp. 1280-1292, DOI: [10.28991/ESJ-2024-08-04-03](https://doi.org/10.28991/ESJ-2024-08-04-03)
- [20] A.C. Manalo, E. Wani, N.A. Zukarnain, W. Karunasena, K.-t. Lau, Effects of alkali treatment and elevated temperature on the mechanical properties of bamboo fibre-polyester composites, *Composites Part B: Engineering*, Vol. 80, 2015, pp. 73-83, DOI: [10.1016/j.compositesb.2015.05.033](https://doi.org/10.1016/j.compositesb.2015.05.033)
- [21] Y. Qin, S. Zhang, X. Wei, Study on friction mechanism and performance of disc brakes for mining motor vehicle, *Mathematical Models in Engineering*, Vol. 4, No. 1, 2018, pp. 11-17, DOI: [10.21595/mme.2018.19678](https://doi.org/10.21595/mme.2018.19678)

- [22] F.N. Ajjan, M.J. Jafari, T. Rebiš, T. Ederth, O. Inganäs, Spectroelectrochemical investigation of redox states in a polypyrrole/lignin composite electrode material, *Journal of Materials Chemistry A*, Vol. 3, No. 24, 2015, pp. 12927-12937, DOI: [10.1039/C5TA00788G](https://doi.org/10.1039/C5TA00788G)
- [23] S.M. Jasim, N.A. Ali, S.I. Hussein, A. Al Bahir, N.S. Abd El-Gawaad, A. Sedky, A.M. Mebed, A.M. Abd-Elnaiem, Enhancement of mechanical properties, wettability, roughness, and thermal insulation of epoxy-cement composites for building construction, *Buildings*, Vol. 15, No. 4, 2025, Paper 643, DOI: [10.3390/buildings15040643](https://doi.org/10.3390/buildings15040643)
- [24] S. Hofmann, T. Lohner, K. Stahl, Influence of water content on elastohydrodynamic friction and film thickness of water-containing polyalkylene glycols, *Frontiers in Mechanical Engineering*, Vol. 9, 2023, Paper 1128447, DOI: [10.3389/fmech.2023.1128447](https://doi.org/10.3389/fmech.2023.1128447)
- [25] K. Yu, X. Shang, X. Zhao, L. Fu, X. Zuo, H. Yang, High frictional stability of braking material reinforced by basalt fibers, *Tribology International*, Vol. 178, No. A, 2023, Paper 108048, DOI: [10.1016/j.triboint.2022.108048](https://doi.org/10.1016/j.triboint.2022.108048)
- [26] M. Babić, B. Stojanović, S. Mitrović, I. Bobić, N. Miloradović, M. Pantić, The influence of lubricant on friction coefficient of hybrid Al-SiC-Gr composites, *Tribological Journal BULTRIB*, Vol. 3, 2013, pp. 148-154.
- [27] N.W. Khun, E. Liu, Tribological behavior of polyurethane immersed in acidic solution, *Tribology Transactions*, Vol. 55, No. 4, 2012, pp. 401-408, DOI: [10.1080/10402004.2012.656881](https://doi.org/10.1080/10402004.2012.656881)
- [28] Q. Gao, P. Wei, K. Li, L. Fang, Q. Li, Z. Wu, Y. Wan, Y. Feng, D. Wang, New castor oil-based green conductive gel lubricant featuring with ultra low friction coefficient of 0.038, *Applied Surface Science*, Vol. 708, 2025, Paper 163715, DOI: [10.1016/j.apsusc.2025.163715](https://doi.org/10.1016/j.apsusc.2025.163715)
- [29] V.I. Kolesnikov, N.A. Myasnikova, F.V. Myasnikov, M.V. Boiko, E.S. Novikov, V.V. Avilov, Physicomechanical and tribological properties of polymer composites filled with lubricant-containing microcapsules, *Russian Journal of Applied Chemistry*, Vol. 91, No. 10, 2018, pp. 1617-1625, DOI: [10.1134/S1070427218100087](https://doi.org/10.1134/S1070427218100087)
- [30] P. Sabarinathan, K. Rajkumar, V.E. Annamalai, K. Vishal, Characterization on chemical and mechanical properties of silane treated fish tail palm fibres, *International Journal of Biological Macromolecules*, Vol. 163, 2020, pp. 2457-2464, DOI: [10.1016/j.ijbiomac.2020.09.159](https://doi.org/10.1016/j.ijbiomac.2020.09.159)
- [31] A.S. Syahrani, A. Sam, Basri, The effect of immersion with time and water variations on bending strength of malapoga wood (*Toona Ciliata M. Roem*), *MATEC Web of Conferences*, Vol. 331, 2020, Paper 05003, DOI: [10.1051/mateconf/202033105003](https://doi.org/10.1051/mateconf/202033105003)
- [32] Y. Bagaiskov, Effect of fluid media on abrasive polymeric composite products with various elasticity, *E3S Web of Conferences*, Vol. 371, 2023, Paper 03010, DOI: [10.1051/e3sconf/202337103010](https://doi.org/10.1051/e3sconf/202337103010)
- [33] A. Afzal, M.K. Bangash, A. Hafeez, K. Shaker, Aging effects on the mechanical performance of carbon fiber-reinforced composites, *International Journal of Polymer Science*, Vol. 2023, 2023, Paper 4379307, DOI: [10.1155/2023/4379307](https://doi.org/10.1155/2023/4379307)
- [34] A.K. Haldar, T. Gobikannan, A. Portela, C. Athavale, A.J. Comer, Mechanical characterization of polymer composite materials for long length ships, in *Proceedings of the International Conference on Marine Design 2020*, 15-16.01.2020, Cádiz, Spain, pp. 121-124.
- [35] N. Nosbi, H.M. Akil, Z.A. Mohd Ishak, A.A. Bakar, Effect of water absorption on the mechanical properties of pultruded kenaf fibre reinforced polyester composites, *Advanced Composites Letters*, Vol. 20, No. 1, 2011, DOI: [10.1177/096369351102000103](https://doi.org/10.1177/096369351102000103)
- [36] M. Barczewski, J. Cyganek, D. Matykiewicz, J. Andrzejewski, The impact of engine oil and windshield washer fluid exposure on the structure and properties of injection-molded nucleated polylactide-basalt composites, *Arabian Journal for Science and Engineering*, Article in Press, DOI: [10.1007/s13369-025-10269-9](https://doi.org/10.1007/s13369-025-10269-9)
- [37] E. Hozdić, E. Hozdić, Comparative analysis of the influence of mineral engine oil on the mechanical parameters of FDM 3D-printed PLA, PLA+CF, PETG, and PETG+CF materials, *Materials*, Vol. 16, No. 18, 2023, Paper 6342, DOI: [10.3390/ma16186342](https://doi.org/10.3390/ma16186342)
- [38] A.M. Amaro, M.F. Paulino, M.A. Neto, P.N.B. Reis, Hardness and roughness of glass/epoxy composite laminates subjected to different hostile solutions: A comparative study, *Polymers*, Vol. 17, No. 7, 2025, Paper 993, DOI: [10.3390/polym17070993](https://doi.org/10.3390/polym17070993)
- [39] S. Jayakrishnan, G. Ragul, Effect of mechanical properties of composite material under the influence of different commercial oils, *International Journal of Innovative Research in Technology*, Vol. 2, No. 8, 2016, pp. 60-66.
- [40] A.A. Mohammed, T.T. Issa, The water absorption effect on the hardness of composites polyester, *AIP Conference Proceedings*, Vol. 1727, 2016, Paper 020016, DOI: [10.1063/1.4945971](https://doi.org/10.1063/1.4945971)